ISSN 0018-1439, High Energy Chemistry, 2017, Vol. 51, No. 4, pp. 245–249. © Pleiades Publishing, Ltd., 2017.
Original Russian Text © E.B. Gordon, A.V. Karabulin, S.A. Krasnokutski, V.I. Matyushenko, I.I. Khodos, 2017, published in Khimiya Vysokikh Energii, 2017, Vol. 51, No. 4, pp. 261–265.

Formation of Nanostructures during Coagulation of Semiconductors in Superfluid Helium

E. B. Gordon[a], *, A. V. Karabulin[b], S. A. Krasnokutski[c], V. I. Matyushenko[d], and I. I. Khodos[e]

[a] *Institute of Problems of Chemical Physics, Russian Academy of Sciences, Chernogolovka, Moscow oblast, Russia*
[b] *MEPhI National Research Nuclear University (Moscow Institute of Engineering Physics), Moscow, Russia*
[c] *Laboratory Astrophysics Group of the Max Planck Institute for Astronomy at the Friedrich Schiller University Jena, Institute of Solid State Physics, Helmholtzweg 3, D-07743 Jena, Germany*
[d] *Talrose Institute of Energy Problems of Chemical Physics, Chernogolovka Branch, Russian Academy of Sciences, Chernogolovka, Moscow oblast, Russia*
[e] *Institute of Problems of Technology in Microelectronics and Ultrahigh-Purity Materials, Russian Academy of Sciences, Chernogolovka, Moscow oblast, Russia*
**e-mail: gordon@ficp.ac.ru*

Received December 1, 2016

Abstract—As in the case of metals, laser ablation of germanium and silicon in superfluid helium leads to the formation of thin nanowires; spherical nanoclusters are also present in ablation products. A decrease in the resistance of bundles of silicon nanowires with increasing temperature is typical of semiconductors. Laser ablation of amorphous graphite also leads to the formation of quasi-one-dimensional structures, but there are no spherical clusters among the coagulation products. The structure of carbon filaments is amorphous; they contain onion-like entities, and nanodiamonds appear as coagulation products when the concentration of carbon introduced into superfluid helium increases. The peculiar behavior of carbon is associated with the impossibility of its melting at low pressures.

Keywords: superfluid helium, laser ablation, nanowires, nanodiamonds
DOI: 10.1134/S001814391704004X

INTRODUCTION

Using the bottom-up synthesis of nanowires based on laser ablation of a metal in superfluid helium (He II) which we had developed [1, 2], thin high-quality nanowires of many metals and their binary alloys were prepared and studied [3–6]. The method is based on the previously discovered process of coagulation of impurities in quantized vortices of superfluid helium [7, 8]. The mechanism of nanowire formation is a sequence of the following processes, which occur almost adiabatically owing to the specifics of heat transfer in He II [9, 10]. The primary products of laser ablation at energy densities used are atoms, dimers, and clusters containing up to several tens of atoms. All impurity particles are entrained into the core of quantized vortices present in He II. In the first stage of coagulation, collisions lead to growth of the clusters, with the energy released by reducing the total surface being sufficient to melt the resulting larger clusters. The molten metal acquires a spherical shape due to surface tension. This scenario continues until the cluster size increases to such an extent that the heat released during coagulation becomes insufficient to melt the coagulation product. After that, the clusters can only fuse together, forming elongated entities oriented along the axis of the quantized vortex. According to the mechanism proposed in [9], this critical size, which is different for different metals, determines the diameter of the nanowire that grows inside the quantized vortices.

All these processes are nonspecific; they must proceed for any atoms, molecules, and nanoparticles. Since all the processes involved in the mechanism are universal (vortex affinity depends mainly on the cluster size, since this is the Bernoulli force; probably, the motion along the vortex is also independent of the nature of the substance), a natural question arises whether this method can be used to obtain nanostructures, namely nanowires, nanospheres, and microspheres, from semiconductors. This task is no less demanding than the fabrication of metallic nanowires and nanospheres, since semiconductors form the basis of modern electronics and are actively used in many fields of nanotechnology. Quasi-one-dimensional nanosized heterostructures which consist of various semiconductors or semiconductor–metal structures are also of interest. These considerations have given an impetus to the present study in which the products of coagulation of semiconductors in superfluid helium are studied experimentally.

Characteristics of the objects of study. T_{melt} is the melting point, P_{sv} is the saturated vapor pressure above the melt at the melting point, T_{ad} is the adiabatic heating temperature of the product when two nanoclusters with a diameter of 1 nm are merged, and R_{nw} is the nanowire radius calculated from Eq. (8) reported in [9]. The initial data reported in [11]

Substance	T_{melt}, K	P_{sv}, Pa	T_{ad}, K	R_{nw}, nm
Germanium	1210	1.3×10^{-4}	3370	1.8
Silicon	1696	6.7	4180	1.6
Carbon	4500–5000*	$\approx 10^7$	>10000	1.5

* The exact value of the melting point of carbon is unknown, the range specified is taken from [12].

EXPERIMENTAL

In our experiments, we used the previously described setup [1, 9] and standard procedures for the creation and study of nanostructures. Nanowires were grown in an optical cryostat under superfluid helium at a temperature of about 1.7 K. Laser ablation of the targets immersed in He II was carried out through a sapphire window with a focused beam of a solid state Nd : LSB laser focused on the target, which has the following characteristics: wavelength $\lambda = 1.062$ μm, pulse energy $E = 0.1$ mJ, pulse duration $\tau = 0.5$ ns, and pulse repetition frequency $f = 4000$ Hz. The spot diameter at the laser focus was about 100 μm. Plates of reagent grade materials were used as targets.

The main part of the condensation products settled to the bottom of the experimental cells, which accommodated in special holders grids of a 3 mm diameter made of thin metal wires (gold or copper) coated with a perforated carbon film generally used in transmission electron microscopic (TEM) analysis. After heating the samples to room temperature, the grids were transferred to the electron microscope chamber.

Another part of the nanowires closed the vertical line of the gilded electrodes (interelectrode distance 1.5 mm) located at a distance of 1–1.5 cm from the target. This arrangement made it possible to study the electric conductivity of nanowires directly in a cryostat in an inert helium medium within the temperature range of 1.5–300 K. The conductivity was measured using a Keithley 2000 digital multimeter. The recording system made it possible to simultaneously measure the resistance of three different bundles of nanowires in the automatic mode.

OBJECTS OF STUDY

Three most popular semiconductors were chosen as the objects of the study. These were silicon and germanium, which play an exceptional role in microelectronics and nanophotonics, and carbon, which is no less interesting in connection with its many allotropic forms and unique types of nanostructures, such as nanotubes, fullerenes, graphenes, and nanodiamonds.

The table lists certain thermochemical properties of these elements and the expected radii of nanowires as calculated by the equations given in [9]. Germanium plates of a 2 mm thickness and silicon plates of a 0.5 mm thickness were used as targets. The carbon target was a amorphous graphite plate with a thickness of 3 mm (laser ablation of crystalline graphite led to the splitting of submicron-sized flakes consisting of several layers).

Although the thermophysical properties of carbon at high temperatures have not been well documented [12], it is absolutely clear that the saturated vapor pressure at the carbon melting point significantly exceeds the atmospheric pressure regardless of whether this point is at 4500 [13] or 5000 K [14]. For comparison, the saturated vapor pressure over liquid metals at $T = T_{melt}$ does not exceed 200 Pa for refractory metals (tungsten or niobium) and lies in the range of 10^{-6}–10^{-2} Pa for more fusible metals (gold or copper). For germanium and silicon, these values approximately correspond to those for metals (table).

This puts carbon in very special conditions from the point of view of coagulation of its nanoclusters in superfluid helium. The mechanism described in the introduction is untrue for it, since carbon clusters cannot ever melt in superfluid helium. A significant increase in temperature during coagulation does take place, but long before the melting point is reached, the pressure of saturated carbon vapor above the surface of the solid carbon cluster becomes so large that the gas shell filled with high-pressure carbon vapor ceases to be a heat insulator. At the same time, the temperature of solid carbon clusters can be very high; for example, the saturated vapor pressure of carbon becomes 10 Pa only at $T = 3200$ K. At these temperatures, the surface mobility of carbon atoms is already sufficiently high [15], but clusters can hardly acquire a spherical shape because of it. Interestingly, unlike metals (or germanium and silicon), the temperature of carbon clusters inside He II is determined by the pressure of its saturated vapor and should not be a strong function of the cluster size.

RESULTS AND DISCUSSION

Figures 1 and 2 show microphotographs of ablation products of germanium and silicon, respectively, obtained using a Jeol JEM-2100 transmission electron microscope. In principle, both the morphology and

structure of the coagulation products of both semiconductors are similar to those obtained for metals [3–5, 9, 10]. As in the case of metals, the condensation product is a crosslinked three-dimensional nanoweb; in addition to nanowires, spherical particles of regular shape are formed. A significant difference is that a large number of nanospheres with a diameter of about 10 nm are embedded in nanowires, and the lengths of individual nanowires in nanoweb are as small as about 100 nm.

The results obtained are not unexpected. Indeed, as already has been mentioned in the introduction, laser ablation occurs at cryogenic temperatures of the sample, i.e. under conditions of low thermal conductivity of semiconductors (at these temperatures, the electronic part of the thermal conductivity disappears in semiconductors and only the lattice thermal conductivity remains). In this sense, they conduct heat as dielectrics, and during the laser pulse, a much thinner layer of the sample is heated than in the case of metals. As a result, the semiconductor absorbs significantly more heat per unit volume at the same laser pulse parameters than the metal, thereby sharply reducing the ablation threshold. Indeed, the amount of substance absorbed in a single laser pulse in the case of semiconductors is much higher than in the case of metals. According to the mechanism proposed in [9], the formation of spherical particles of a comparatively large size was explained by large metal densities inside superfluid helium, when collisions of the clusters that have not cooled to helium temperatures are possible. Naturally, since the density of the compound suspended in helium for semiconductors is higher as compared with metals, the contribution of the reaction route leading to the formation of spheres is greater for them.

To judge whether thin nanowires made of a semiconductor chemical element retain its semiconducting properties, we used the above-described procedure for studying the electrical properties of nanowires.

For metals, the dependence of the resistance of the nanowire bundle on the temperature measured in the cryostat was very weak. This was explained [16] by the fact that in thin nanowires, the main losses are not the scattering of conduction electrons by phonons, but their temperature-invariant scattering on the surface of nanowires. In metals, the number of charge carriers and, hence, the resistance of metallic nanowires are also independent of temperature.

At the same time, as can be seen from Fig. 3, the resistance of a bundle of nanowires falls rather strongly with the increasing temperature. This behavior is typical for semiconductor nanowires. Indeed, in semiconductors, the scattering of conduction electrons takes place on the surface of the wires and, therefore, does not depend on temperature; however, the number of charge carriers in them exponentially increases with temperature. The result obtained demonstrates that thin nanowires made of silicon retain the semiconductor electrical properties.

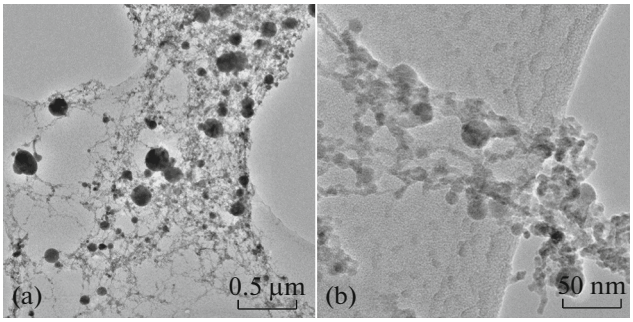

Fig. 1. (a) Morphology and (b) structure of germanium ablation products.

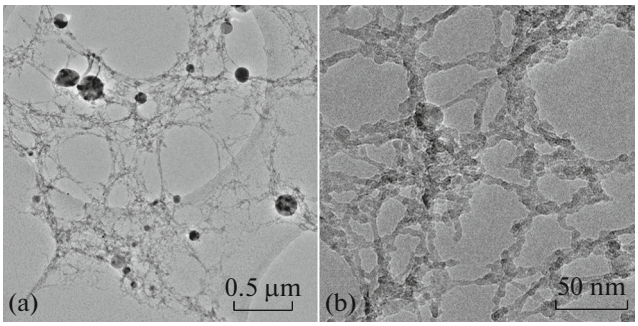

Fig. 2. (a) Morphology and (b) structure of silicon ablation products.

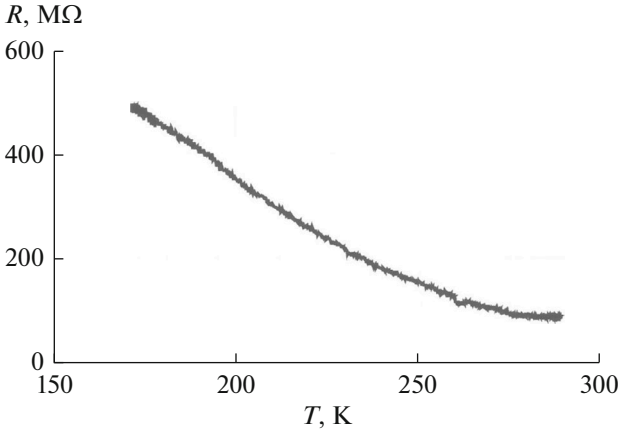

Fig. 3. Resistance of a bundle of silicon nanowires as a function of temperature.

The most interesting were the results for nanostructures formed during laser ablation of amorphous carbon. Since the micrographs obtained with the JEOL JEM-2100 electron microscope showed low contrast in the case of carbon, electron microscopy of the samples obtained at the Institute of Problems of

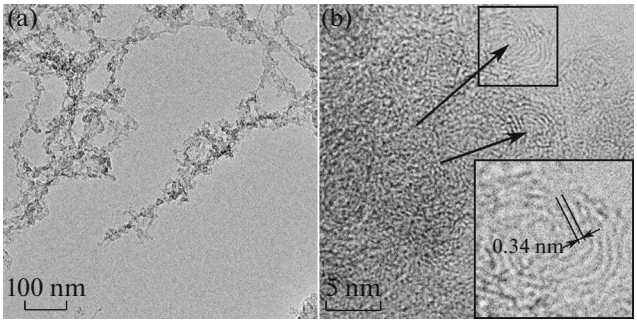

Fig. 4. (a) Morphology and (b) structure of carbon ablation products obtained on a Jeol JEM 3010 high-resolution transmission electron microscope (Germany, Jena).

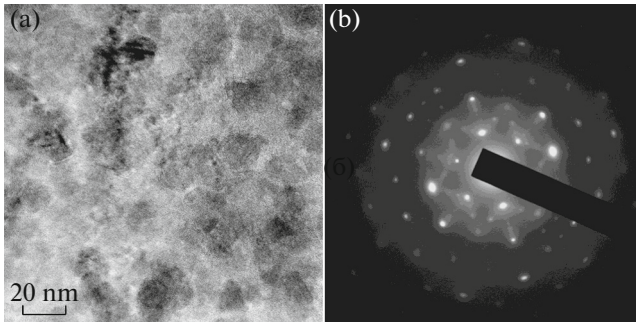

Fig. 5. Structure and electron diffraction pattern of carbon products obtained on a Jeol JEM-2100 transmission electron microscope (Russia, Chernogolovka).

Chemical Physics was carried out at the University of Jena. At the University of Jena, the examination was carried out in the transmission mode using a Jeol JEM 3010 high-resolution electron microscope with a LaB_6 cathode operating at a voltage of 300 kV and allowing energy-dispersive X-ray spectroscopy to determine the chemical composition of the sample. In this way, the required high contrast and spatial resolution was achieved. Typical micrographs of nanostructures are shown in Fig. 4. It can be seen that carbon forms short needles with a thickness of 10 nm; however, there are no spherical clusters for it, both large and small, which are included in the composition of "wires" in the case of germanium and silicon (they are absent not only in the fragment shown in Fig. 4b, but in the entire sample). The structure of the needles is of particular interest; they are an amorphous carbon containing "onions" or nested fullerenes. Although they are not regular spheres, the distances between layers are close to 0.34 nm typical of the carbon "onions" [17], and their presence unambiguously indicates that the temperatures were high during the condensation. the onion-like structures are entities close to nanodiamonds; at least, it is known that they reversibly transform into each other [17, 18].

The complete absence of spherical particles in carbon samples is an important piece of evidence for the statement advanced in [9] that sufficiently large spheres are formed during the coalescence of hot nanoclusters accompanied by melting. Indeed, there is no melting in the carbon, so there should be no spheres. In addition, the relatively large (in comparison with the predictions of the table) needle diameters can be explained by the absence of a critical cluster size for carbon, above which there is no melting of the product during coagulation; therefore, none of the clusters undergoes melting.

Since the probability of mutual collisions increases with increasing concentration of the substance introduced into superfluid helium, we decided to increase the energy of the laser pulse in order to increase the efficiency of the formation of spherical particles. In these experiments, an YLP-170/2/12 pulsed ytterbium fiber laser with an emission wavelength of $\lambda = 1.062$ μm, an energy per pulse of up to $E = 0.21$ mJ, a pulse duration of $\tau = 20$ ns, and a pulse repetition rate of $f = 500-2000$ Hz was used. The thermal conductivity of graphite is low at low temperatures; the use of a laser with a longer pulse should not increase the ablation threshold. Indeed, the yield of carbon evaporating in a single laser pulse has increased, and the main coagulation product of steel, as seen in Fig. 5a, is grains with a size of 20–30 nm. An electron diffraction pattern taken using a diaphragm 500 nm in diameter showed that these grains are slightly disoriented diamonds (see Fig. 5b).

CONCLUSIONS

The experiments described in this paper confirmed that for semiconductors, as well as for metals, the quantized vortices in superfluid helium are a universal template determining the growth of the coagulation product of particles introduced into it, exclusively in one direction. In this sense, nanowires must be obtained for any substance suspended in a liquid. However, for nanofilaments produced by coagulation to have a regular shape and dense structure, the nanowire should be formed from molten protoclusters. To provide these conditions in superfluid helium, in addition to the requirements of energy release during coagulation being sufficient for melting, it is necessary that the saturated vapor pressure over the substance in the molten state be no more than a few pascals. Otherwise, the nanostructures grown in superfluid helium will have a loose, fractal structure. In this case, no spherical nanoparticles will be formed.

Fortunately, both germanium and silicon, like all metals, are characterized by a low saturated vapor pressure above the melt. Therefore, thin nanowires and nanosized heterostructures of regular shape and close packing can be grown for them and their alloys.

ACKNOWLEDGMENTS

This work was supported by the Russian Science Foundation, grant no. 14-13-00574.

REFERENCES

1. Gordon, E.B., Karabulin, A.V., Matyushenko, V.I., Sizov, V.D., and Khodos, I.I., *Low Temp. Phys.*, 2010, vol. 36, p. 590.
2. Moroshkin, P., Lebedev, V., Grobety, B., Neururer, C., Gordon, E.B., and Weis, A., *EPL*, 2010, vol. 90, p. 34002.
3. Gordon, E.B., Karabulin, A.V., Matyushenko, V.I., Sizov, V.D., and Khodos, I.I., *Phys. Chem. Chem. Phys.*, 2014, vol. 16, p. 25229.
4. Gordon, E.B., Karabulin, A.V., Morozov, A.A., Matyushenko, V.I., Sizov, V.D., and Khodos, I.I., *J. Phys. Chem. Lett.,* 2014, vol. 5, p. 1072.
5. Gordon, E.B., Karabulin, A.V., Matyushenko, V.I., Sizov, V.D., and Khodos, I.I., *Laser Phys. Lett.*, 2015, vol. 12, p. 096002.
6. Gordon, E.B., Karabulin, A.V., Matyushenko, V.I., Sizov, V.D., Rostovshchikova, T.N., Nikolaev, S.A., Lokteva, E.S., Golubina, E.V., Maslakov, K.I., Krotova, I.N., Gurevich, S.A., Kozhevin, V.M., and Yavsin D.A., *High Energy Chem.*, 2016, vol. 50, p. 292.
7. Gordon, E.B., Nishida, R., Nomura, R., and Okuda, Y., *JETP Lett.*, 2007, vol. 85, p. 581.
8. Gordon, E.B. and Okuda, Y., *J. Low Temp. Phys.*, 2009, vol. 35, no. 3, p. 209.
9. Gordon, E.B., Karabulin, A.V., Matyushenko, V.I., Sizov, V.D., and Khodos, I.I., *JETP*, 2010, vol. 112, p. 1061.
10. Gordon, E.B., Karabulin, A.V., Matyushenko, V.I., Sizov, V.D., and Khodos, I.I., *High Energy Chem.*, 2014, vol. 48, p. 206.
11. *Spravochnik: Tablitsy fizicheskikh velichin* (Handbook of Physical Quantities), Kikoin, I.K., Ed., Moscow: Atomizdat, 1976.
12. Savvatimskii, A.I., *Usp. Fiz. Nauk*, 2003, vol. 173, no. 12, p. 1371.
13. Cezairliyan, A. and Muller, A.P., *Int. J. Thermophys.*, 1990, vol. 11, p. 643.
14. Baitin, A.V., Lebedev, A.A., Romanenko, S.V., Senchenko, V.N., and Sheindlin, M.A., *High Temp.–High Pressures*, 1990, vol. 22, p. 157.
15. Gordon, E.B., Karabulin, A.V., Matyushenko, V.I., Rostovshchikova, T.N., Nikolaev, S.A., and Lokteva, E.S., *Theor. Exp. Chem.*, 2016, vol. 52, p. 75.
16. Gordon, E.B., Karabulin, A.V., Matyushenko, V.I., Sizov, V.D., and Khodos, I.I., *Appl. Phys. Lett.*, 2012, vol. 101, p. 052605.
17. Wesolowski, P., Lyutovich, Y., Banhart, F., Carstanjen, H.D., and Kronmuller, H., *Appl. Phys. Lett.*, 1997, vol. 71, p. 1948.
18. Banhart, F., *J. Appl. Phys.*, 1997, vol. 81, p. 3440.

Translated by V. Avdeeva